CrossMark

ORIGINAL PAPER

High-resolution WRF simulation of cloud properties over the super typhoon Haiyan: physics parameterizations and comparison against MODIS

Tanvir Islam[1] · Prashant K. Srivastava[2,3] · Qiang Dai[4]

Abstract Numerical weather prediction (NWP) models can complement the satellite technology in simulating the cloud properties, especially in extreme storm events, when gathering new data becomes more than essential for accurate weather forecasting. In this study, we investigate the capability of the Weather Research and Forecasting (WRF) model to realistically simulate some important cloud properties in high-resolution grids, such as cloud phase (e.g., liquid or ice) and cloud water path. The sensitivity of different combinations of physics parameterizations to the simulated cloud fields is studied. The experiment is conducted on a super typhoon event by configuring the WRF model in two domains, with two-way nesting, allowing bidirectional information exchange between the parent and the nest. In order to do the assessment, the simulated cloud fields are compared against MODIS-derived cloud properties from one overpass scene. While the simulations have been able to capture the spatial distribution of cloud properties reasonably well, produced cloud quantities such as ice water path has been significantly overestimated when compared to the MODIS optical cloud information. The microphysics parameterizations are found to be more sensitive than the planetary boundary layer (PBL) parameterizations.

✉ Tanvir Islam
tanvir.islam@jpl.nasa.gov

[1] NASA Jet Propulsion Laboratory, California Institute of Technology, Pasadena, CA, USA

[2] NASA Goddard Space Flight Center, Greenbelt, MD, USA

[3] Earth System Science Interdisciplinary Center, University of Maryland, College Park, MD, USA

[4] Department of Civil Engineering, University of Bristol, Bristol, UK

1 Introduction

From weather forecasting perspective to radiative energy balance standpoint, gathering accurate information on cloud properties is important on a day-to-day basis. Clouds are also principal modulators of the earth's hydrological cycle connecting a critical link between precipitation efficiency and radiative budget of the climate system. They also play a crucial role in the formation of severe storms by condensing water vapor from warm ocean to form large cumulonimbus clouds.

The cloud properties such as thermodynamic phase of clouds (e.g., liquid/ice) and their quantities can generally be measured by ground-based or satellite-borne remote-sensing instruments. In particular, good efforts have been made to derive cloud quantities from the measurements on-board various satellite platforms. Both passive and active remote-sensing techniques have been successful in providing a good insight into the distribution of clouds over both ocean and land surfaces. Some of the prior studies related to satellite observation of clouds are documented in Otkin and Greenwald (2008), Minnis et al. (2011), Islam et al. (2014a), and Islam et al. (2014d), and can be referred therein.

Nevertheless, satellite data are scarce and have temporal and spatial resolution limitations. On the other hand, cloud quantities change rapidly and vary with respect to time and space. Therefore, satellite-based estimate of cloud quantities cannot provide a full picture of cloud information of our entire globe. The mesoscale numerical weather prediction (NWP) models can complement the space-based technologies for a variety of atmospheric and surface observations, including clouds. With the advancements in computing powers, it is now possible to simulate weather events in very high resolution, and as such, a wide range of NWP studies is comprehensively

documented in the literature (Dai et al. 2013; Ishak et al. 2013; Islam et al. 2013; Srivastava et al. 2013; Islam et al. 2014b; Srivastava et al. 2014a; Srivastava et al. 2014b). However, the NWP models have their own limitations itself, for instances, the limitations associated with the physics parameterizations used. In order to accurately simulate the cloud morphology in mesoscale models, it is essential to take into account of all complex interactions between cloud species with precise particle size distribution. However, in reality, bulk microphysics schemes are used in mesoscale models with some approximations of particle size distribution. Besides, simulation errors could also be introduced from model initialization, lateral boundary conditions, model resolution, and other physics parameterizations such as planetary boundary layer (PBL) and cumulus schemes.

A tropical cyclone has recently been hit Philippines in November 2013 and has caused a catastrophic damage. The cyclone, named as Haiyan, has had minimum central pressure of 895 hPa, making it one of the strongest typhoons in the history (super typhoon). In the present study, a mesoscale model, known as the Weather Research and Forecasting (WRF), has been used in simulating the clouds over the super typhoon Haiyan. The goal is to evaluate the effect of physics parameterizations on cloud simulation and if they differ with each other. As part of the assessment, the simulated cloud phase (e.g., liquid or ice) and important cloud quantities such as ice water path are compared against MODIS optical cloud information. It is worth mentioning that the simulated track and intensity of the typhoon have been extensively validated in our previous study with the best track data (Islam et al. 2014c). Based on our previous study, it is found that the WRF simulation has been successful in predicting the track propagation of the typhoon. Nevertheless, the model has substantially underestimated the intensity prediction. In this study, we are rather interested in investigating the capability of the WRF model to realistically simulate cloud properties.

The remainder of this paper is structured as follows: The datasets, WRF model configuration, and simulation setup are outlined in Sect. 2. Section 3 provides the results and discussions. The paper is concluded in Sect. 4.

2 Data and simulation setup

2.1 WRF simulation

The Weather Research and Forecasting (WRF) model used in this experiment is the Advanced Research WRF (ARW) dynamic solver, developed by NCAR/MMM (Mesoscale and Microscale Meteorology Division). The equation set for ARW is Eulerian Mass dynamical core with terrain following vertical coordinates. For a comprehensive description of the WRF-ARW dynamic solver, referring the article of Skamarock and Klemp (2008) is recommended to the readers.

In this study, the WRF model is configured to simulate super typhoon Haiyan with two domains, as shown in Fig. 1. Two-way nested run option has been allowed in the simulation between the mother and child domains. The domain 1 (coarse domain) is comprised of 169×135 grid points, 25-km grid size, and 28 vertical levels, covering a size of 4225×3375-km^2 area. The domain 2 is configured using high-resolution grid spacing (5 km), such that small-scale feature of the system can be captured by the model. It covers the area of 2180×2155 km^2, and also uses 28 vertical levels. Note that vertical grids are variable and stretched.

The model topography and other static geo-fields are initialized from very high-resolution global datasets (http://www2.mmm.ucar.edu/wrf). The simulation is performed without assimilating any observation data. The ERA-Interim analyses produced by the ECMWF global forecast model are used for model initialization and lateral boundary conditions. The simulation is started at 0000 UTC 6 November 2013 and run for 48 h. By this time, the system has gained the strength of category 5 equivalent tropical storm.

A variety of physics combinations have been investigated to assess the simulation of cloud properties. Summarizing, a total of 10 simulation experiments have been carried out by employing different physics parameterizations, as tabulated in Table 1. The investigated experiments include a combination
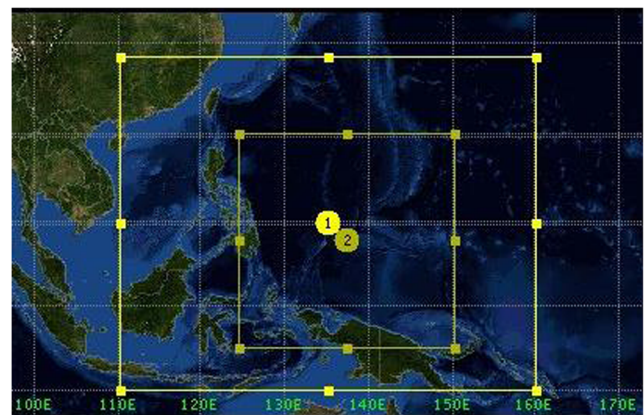

Fig. 1 Map showing the WRF domain settings for the super typhoon Haiyan simulation

Table 1 Physics options used for different simulation experiments

		Microphysics	PBL	Cumulus	Longwave radiation	Shortwave radiation	Surface layer	Land surface
1	GGCE-YSU	GGCE	YSU	KF	RRTM	Dudhia	MM5	Noah
2	MY2-YSU	MY2	YSU	KF	RRTM	Dudhia	MM5	Noah
3	THOM-YSU	THOM	YSU	KF	RRTM	Dudhia	MM5	Noah
4	THOM-YSU-NCu	THOM	YSU	–	RRTM	Dudhia	MM5	Noah
5	WSM3-YSU	WSM3	YSU	KF	RRTM	Dudhia	MM5	Noah
6	WSM6-ACM2	WSM6	ACM2	KF	RRTM	Dudhia	MM5	Noah
7	WSM6-BouLac	WSM6	BouLac	KF	RRTM	Dudhia	MM5	Noah
8	WSM6-MYNN	WSM6	MYNN	KF	RRTM	Dudhia	MM5	Noah
9	WSM6-QNSE	WSM6	QNSE	KF	RRTM	Dudhia	MM5	Noah
10	WSM6-YSU	WSM6	YSU	KF	RRTM	Dudhia	MM5	Noah

of different microphysics and PBL parameterization schemes, including GGCE (Tao et al. 1989), MY2 (Milbrandt and Yau 2005a, b), THOM (Thompson et al. 2008), WSM3 (Hong et al. 2004), WSM6 (Hong and Lim 2006) microphysics schemes, and YSU (Hong et al. 2006), ACM2 (Pleim 2007), BouLac (Bougeault and Lacarrere 1989), MYNN (Nakanishi and Niino 2006), and QNSE (Sukoriansky et al. 2005) PBL schemes. Each simulation uses Kain–Fritsch (KF) cumulus parameterization scheme (Kain 2004), the rapid radiative transfer model (RRTM) longwave radiation scheme, Dudhia shortwave radiation scheme, MM5 similarity surface layer, and Noah land surface model (Chen and Dudhia 2001).

Additionally, a simulation with no cumulus parameterization scheme (THOM-YSU-NCu) is included for comparison with the other simulations.

In the latter section (Sect. 3), we will be comparing the results between different simulations. Furthermore, the simulated cloud properties and cloud quantities will be compared against MODIS-derived outputs.

2.2 MODIS data

The moderate-resolution imaging spectroradiometer (MODIS) is a payload instrument on board the Terra and

Fig. 2 MODIS cloud top pressure (*top left*), cloud top temperature (*top right*), cloud optical thickness (*bottom left*), and cloud phase optical properties (*bottom right*) from the 0120 UTC 7 November 2013 overpass
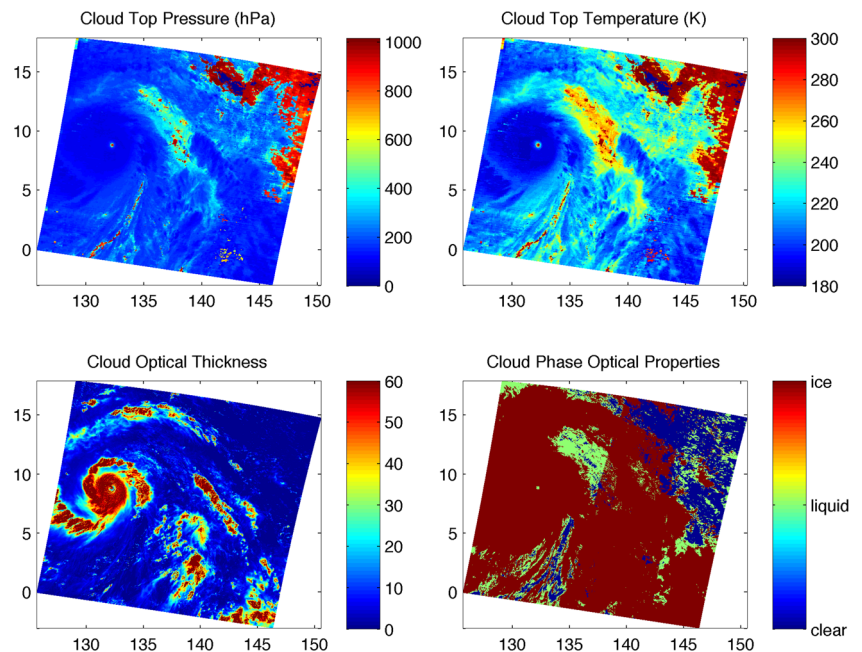
Aqua satellites. It acquires data in 36 spectral bands ranging from 0.4- to 14.4-μm wavelength at varying spatial resolutions. In the present study, the MODIS cloud datasets are acquired from MOD06_L2 atmospheric product. A variety of cloud properties including cloud-particle phase (ice vs. water, clouds vs. snow), effective cloud particle radius (r_e), and cloud optical thickness (τ) are stored in the MOD06_L2 product at 1-km pixel resolution. They are derived using the MODIS visible, near-infrared, and shortwave infrared channel radiances. Cloud water path is then indirectly converted from r_e and τ information. The cloud water path is defined as

$$CWP = \frac{4\rho\tau r_e}{3Q_e} \qquad (1)$$

where CWP can either be liquid water path (LWP) or ice water path (IWP) depending upon the cloud top phase, Q_e is the extinction efficiency, and ρ is the density of water or ice.

Some other cloud properties such as cloud top temperature and cloud top pressure are produced at 5×5 1-km pixel resolution. A complete description of the MODIS cloud algorithms can be found in Platnick et al. (2003).

During our WRF simulation run, a good MODIS overpass scene has been captured by NASA's Terra satellite at 0120 UTC 07 November 2013 over the super typhoon Haiyan. It passed directly over the typhoon region and provided excellent coverage of the model domain. This gives us opportunity to compare the WRF simulated fields against MODIS-derived cloud properties on this particular match-up scene.
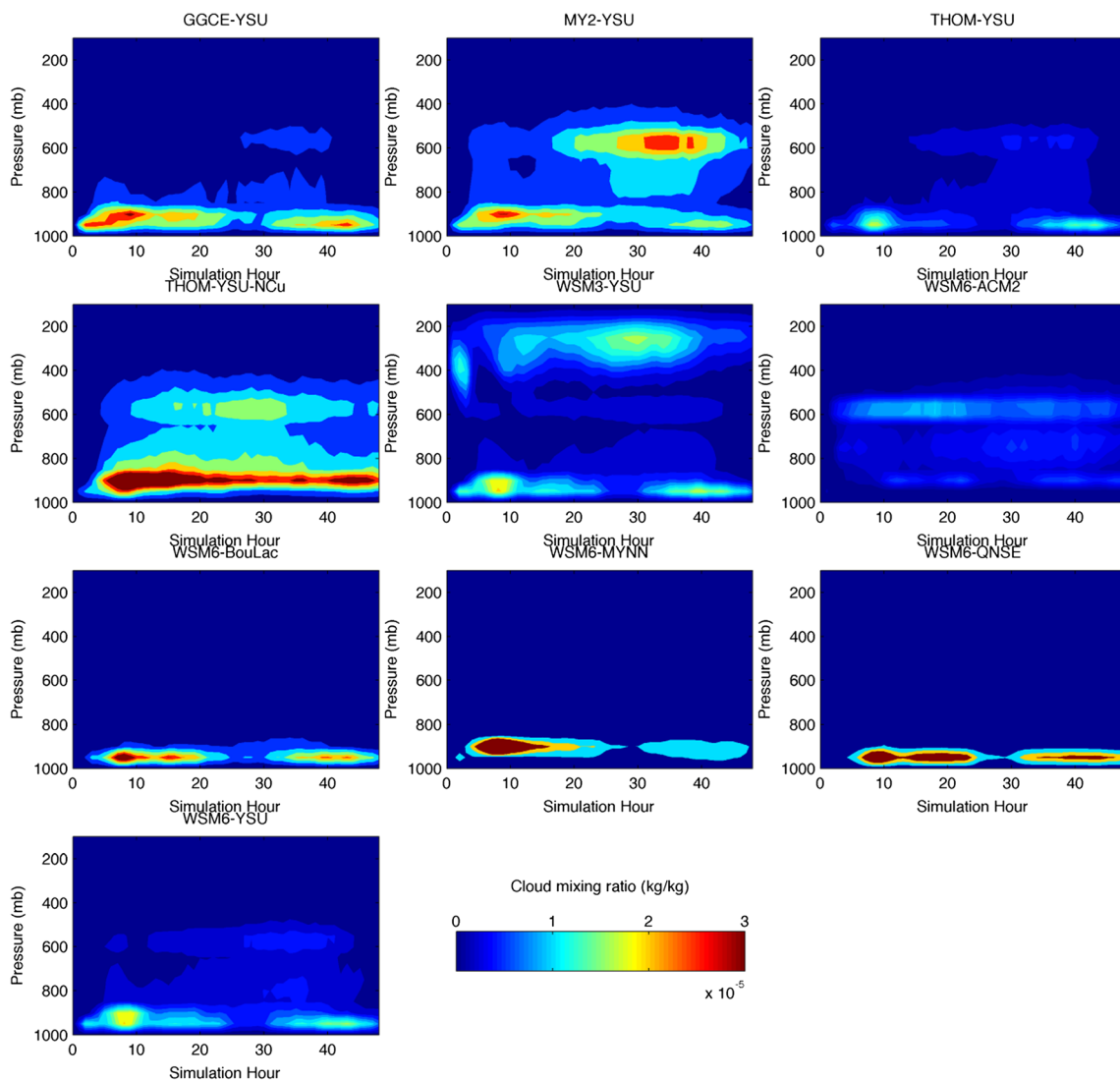

Fig. 3 Evolution of cloud mixing ratio (kg/kg) during the 48-h WRF simulation with different combinations of physics parameterizations from domain 2

Figure 2 highlights some cloud properties as seen by the MODIS instrument for this typhoon overpass. The eye of the cyclone is well depicted in the figure. Generally, in extreme events, such as the event of this tropical cyclone, cloud top pressure should be considerably lower than the vicinity, should have a cold temperature on top of the cloud, and should contain a good amount of ice particles. Such phenomenon is quite evident in this typhoon case, as can be seen from the figure.

3 Results

In this section, we will investigate the variations in simulated cloud properties between the different simulation experiments through the ARW solver. We will also be comparing the simulated cloud information against MODIS overpass data.

Figure 3 depicts the contour diagrams of cloud mixing ratio for the 10 simulation experiments, shown as a function of simulation hours (0–48 h). It is quite certain that the simulation of cloud mixing ratio varies notably among the experiments. Another similar figure is constructed in Fig. 4, but for the rain-mixing ratio. More detailed quantitative comparisons can be made by providing accumulative LWP and IWP amounts for different simulation runs (Fig. 5). As can be seen, the accumulative cloud water path amounts can vary substantially from one physics combination to another one. In particular, the use of different microphysics options can lead to completely different LWP amounts over the entire simulation period. For instance, at the end of 48-h simulation period, more than
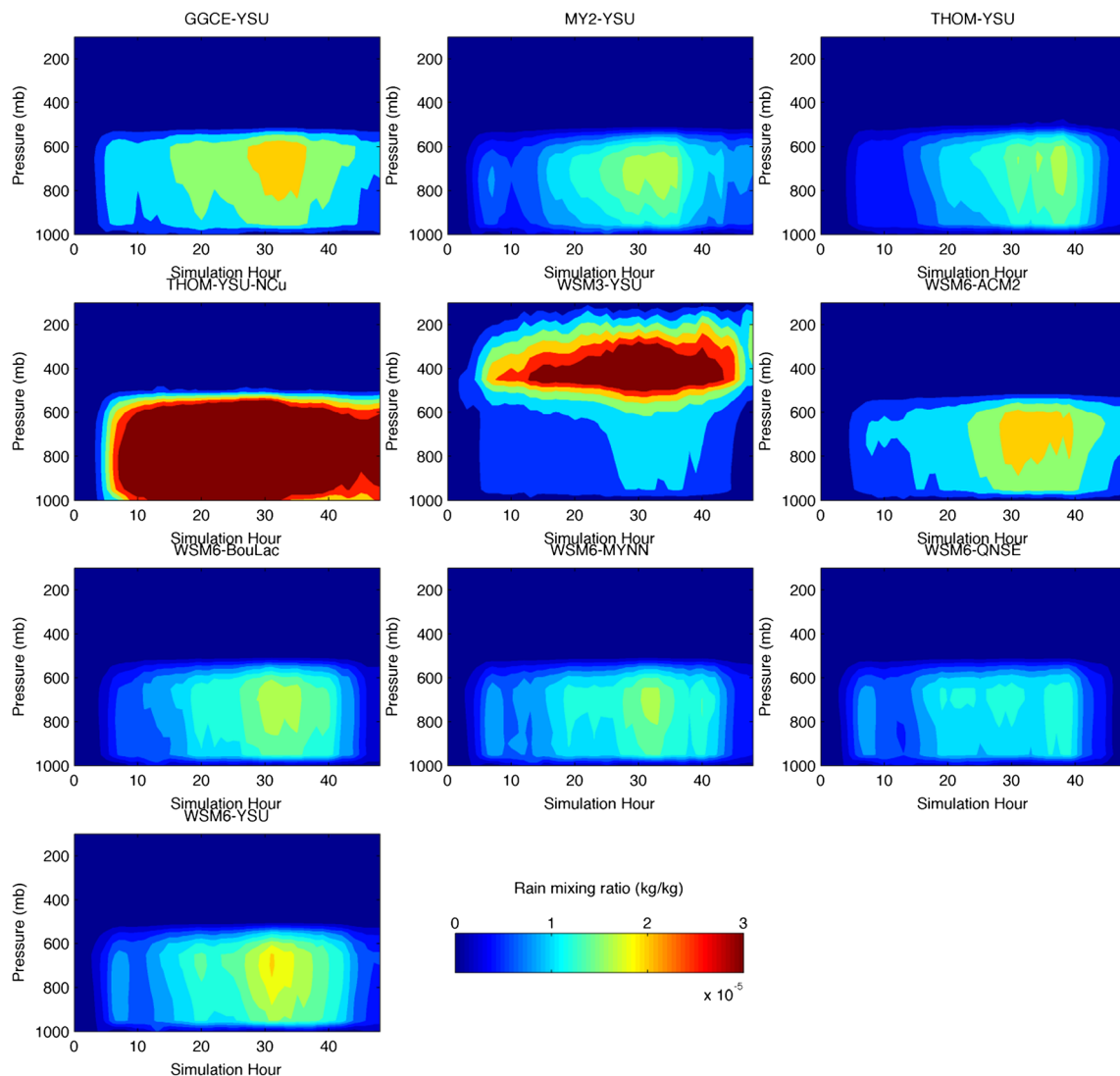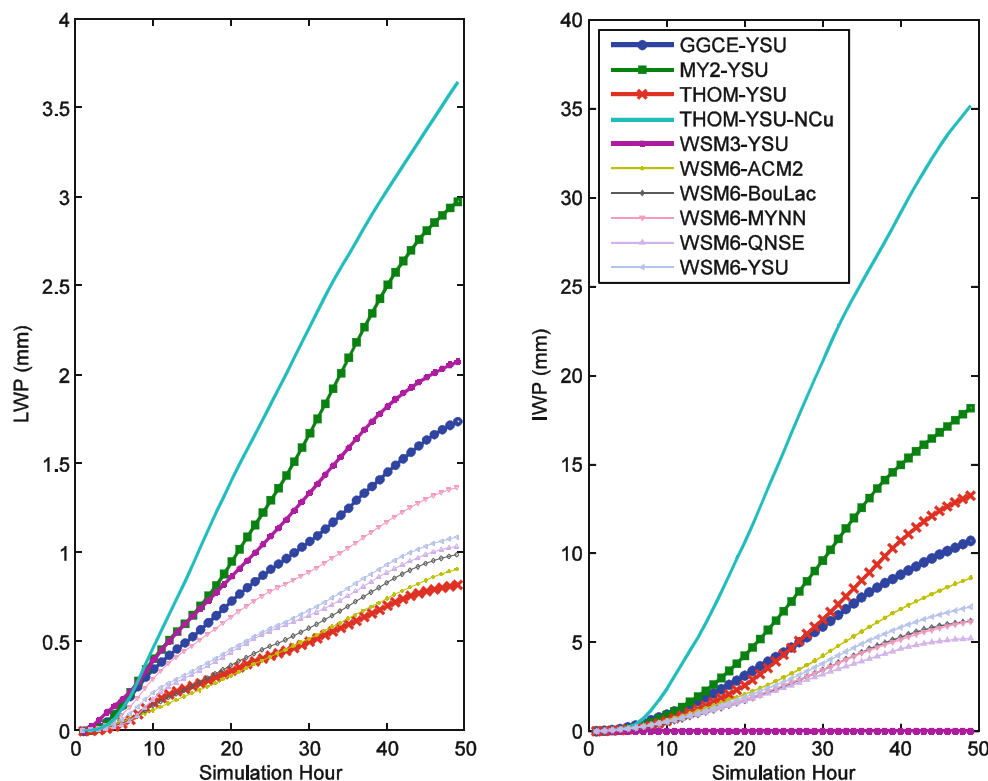

Fig. 4 Same as Fig. 3, but for rain mixing ratio (kg/kg)

Fig. 5 Cumulative LWP (*left*) and IWP (*right*) simulation as a function of simulation hour with different combinations of physics parameterizations

2-mm LWP difference is seen between THOM-YSU and MY2-YSU simulation runs. Note that only dissimilarity between these two runs has been the use of different microphysics options, while other physics options are kept the same. It is also important to outline that the choice for using or not using cumulus parameterizations can play very important role in the simulation results. In our experiments, the THOM-YSU-NCu option, which does not use any cumulus parameterization scheme, has overestimated the LWP quantities than any of the physics combination used. This highlights the importance of using a cumulus parameterization scheme for the cyclonic event simulation. By contrary, the differences in the simulations due to PBL options are relatively small. For the IWP, similar tendencies are seen, demonstrating the lesser variability of IWP amounts between different PBL options (ACM2, BouLac, MYNN, QNSE, YSU with WSM6) than the different microphysics options (GGCE, MY2, THOM, WSM3, WSM6 with YSU). Obviously, WSM3 microphysics parameterization does not use the ice mass variable (Q_i), so IWP cannot be calculated.

In Fig. 6, we provide the WRF simulated IWP fields obtained from the 10 simulation experiments over domain 2 and compare them against MODIS-derived IWP fields. The WRF simulated fields are taken from the closest hours (0100 UTC) to the MODIS overpass time (0120 UTC) on 7 November 2014. For a fair comparison, the MODIS IWP fields are averaged to the WRF domain. All simulation runs reveal a good dynamic structure and location of the cyclone, and, in fact, very close to the field observed by the MODIS. The exception is in the WSM3-YSU case, which has not produced any IWP field due to lack of ice mass variable in the scheme. Apart from this, the WRF model simulates the maturity of the cyclone quite well with realistic coverage of ice clouds. The eye and eyewall of the cyclone are also well produced. Nevertheless, the intensity of the cyclone seems overestimated in terms of IWP amounts, if one attempts to compare the simulation results with MODIS fields. Remarkably, the simulations those used the same microphysics option (WSM6) but different PBL options (ACM2, BouLac, MYNN, QNSE, and YSU) expose very similar IWP fields. Nonetheless, the microphysics options have very strong influence on the spatial coverage of the IWP field. For example, compared to WSM6-YSU simulation, MY2-YSU simulation exerts larger area of geographical coverage. The revealed IWP intensities between these two are also different.
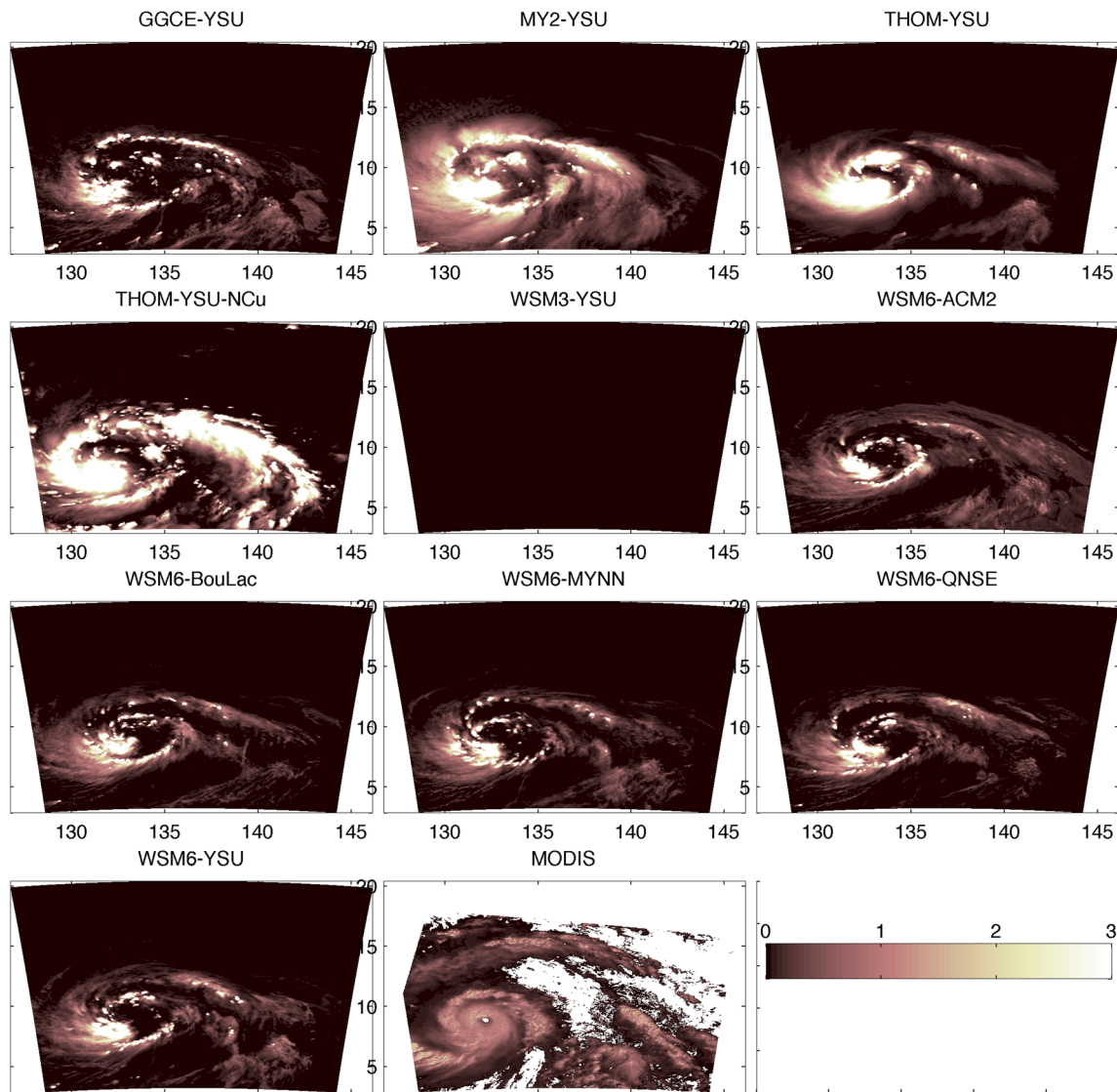
Fig. 6 Simulated IWP (mm) at 0100 UTC on 7 November 2013 with different combinations of physics parameterizations from domain 2. Interpolated MODIS IWP field on the domain is also included for comparison

Furthermore, the THOM-YSU-NCu simulation has produced very high amount of IWP fields, as compared to the other simulation runs. The discrepancies in the magnitudes of the IWP fields can further be visualized through constructing empirical cumulative distribution histograms between the WRF simulated and MODIS-derived IWP fields (Fig. 7). The figure also supports the indication that the greater variability of producing a wide range of IWP magnitudes is mainly associated with the microphysics options, rather than PBL schemes.

Referring to Fig. 2, one can confirm that the selected typhoon event has mainly resulted in ice cloud phase properties in the vicinity of the MODIS overpass granule. Very small spatial precipitation cells are denoted as liquid clouds. Now, we would like to investigate the capability of the WRF model for simulating accurate ice and liquid cloud phase optical properties in comparison with MODIS observations. Table 2 exhibits the percentage of ice and liquid cloud phase cells from the WRF and MODIS datasets over domain 2. It can be seen that 75.93 % pixels are distinguished as ice clouds by the MODIS algorithm in the domain datasets. Only 10.59 % pixels are denoted as liquid pixels. Remaining pixels are associated with clear scenes. In comparison to the

Fig. 7 Empirical cumulative distribution functions of the WRF simulated and the MODIS observed IWP from domain 2
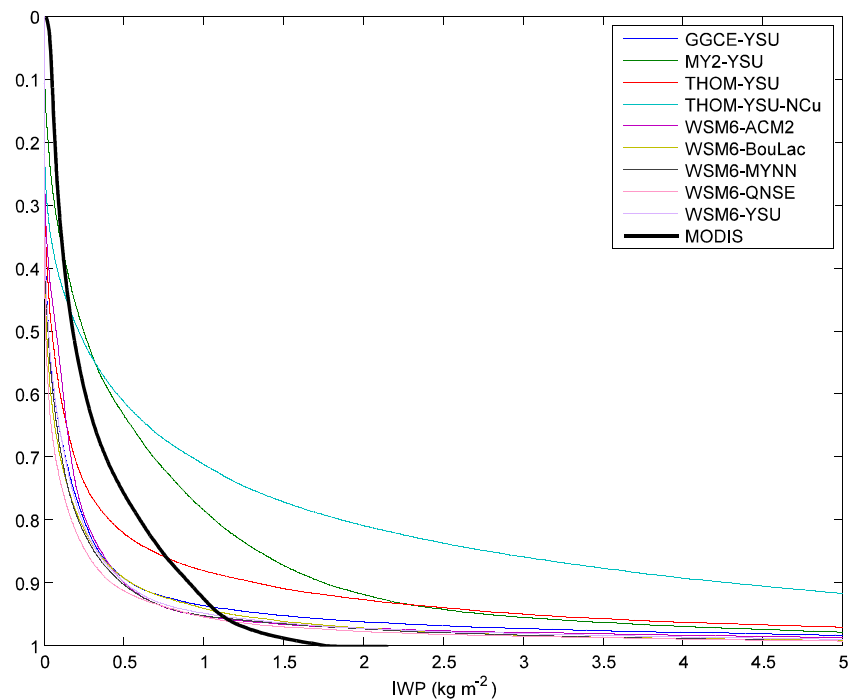
MODIS, WRF simulations contain fewer ice clouds but more liquid clouds. Nevertheless, the frequency range of ice and liquid clouds as simulated by the WRF model over domain 2 by different physics options has appeared to be very comparable. Except for the WSM3-YSU simulation, around 65–68 % pixels are calculated as ice clouds, while 29–37 % pixels are calculated as liquid clouds. In general, the difference between the WRF and the MODIS cloud phase properties can be considered as somewhat reasonable.

Table 2 The WRF and MODIS-derived ice and liquid cloud phase frequencies over the domain 2

	Ice		Liquid	
	WRF	MODIS	WRF	MODIS
GGCE-YSU	67.50 %	75.93 %	30.35 %	10.59 %
MY2-YSU	67.50 %	75.93 %	37.05 %	10.59 %
THOM-YSU	66.35 %	75.93 %	35.13 %	10.59 %
THOM-YSU-NCu	65.96 %	75.93 %	33.51 %	10.59 %
WSM3-YSU	0.00 %	75.93 %	66.79 %	10.59 %
WSM6-ACM2	66.06 %	75.93 %	29.50 %	10.59 %
WSM6-BouLac	66.08 %	75.93 %	32.86 %	10.59 %
WSM6-MYNN	66.81 %	75.93 %	36.73 %	10.59 %
WSM6-QNSE	66.63 %	75.93 %	36.93 %	10.59 %
WSM6-YSU	66.24 %	75.93 %	33.48 %	10.59 %

4 Conclusions

This manuscript examines the capability of a mesoscale NWP model (WRF-ARW) for accurately simulating cloud properties on a tropical cyclonic event over the Northwestern Pacific Ocean. A total of 10 high-resolution simulation experiments have been carried out to investigate the sensitivity of different combinations of physics parameterizations for such simulations. The simulation experiments reveal a strong influence of physics parameterizations on cloud simulation. The variations between the simulated cloud water path amounts have been found very substantial. In particular, such differences are mainly associated with the choice of microphysics parameterizations rather than PBL schemes.

The simulated cloud properties are further compared against MODIS level 2 cloud products. It is found that, in general, the WRF dynamic solver is able to duplicate the realism of cloud fields over the typhoon system. Moreover, the WRF simulated cloud frequencies have agreed reasonably well with the MODIS datasets. Additionally, the use of cumulus parameterization schemes is also essential for good cloud simulation. Nevertheless, the model has been unable to accurately simulate the intensity of the cloud information (e.g., IWP), if one takes the MODIS optical cloud properties as a reference. However, while interpreting the results, one should also remember the obvious difference between MODIS and WRF simulations due to the mismatch of horizontal spatial resolutions. Furthermore, MODIS cloud properties are certainly not true. They are taken as a reference in this work,

but one should consider the uncertainties associated with the MODIS retrievals as well.

Data assimilation can be very useful for improving the WRF simulation and prediction of cloud properties. In the future, we will be investigating whether assimilating satellite radiances could improve the results.

References

Bougeault P, Lacarrere P (1989) Parameterization of orography-induced turbulence in a mesobeta-scale model. Mon Weather Rev 117(8):1872–1890. doi:10.1175/1520-0493(1989)117<1872:pooiti>2.0.co;2

Chen F, Dudhia J (2001) Coupling an advanced land surface-hydrology model with the Penn State-NCAR MM5 modeling system. Part I: model implementation and sensitivity. Mon Weather Rev 129(4):569–585. doi:10.1175/1520-0493(2001)129<0569:caalsh>2.0.co;2

Dai Q, Han DW, Rico-Ramirez MA, Islam T (2013) The impact of raindrop drift in a three-dimensional wind field on a radar-gauge rainfall comparison. Int J Remote Sens 34(21):7739–7760. doi:10.1080/01431161.2013.826838

Hong S-Y, Lim J-OJ (2006) The WRF single-moment 6-class microphysics scheme (WSM6). J Korean Meteor Soc 42(2):129–151

Hong SY, Dudhia J, Chen SH (2004) A revised approach to ice microphysical processes for the bulk parameterization of clouds and precipitation. Mon Weather Rev 132(1):103–120. doi:10.1175/1520-0493(2004)132<0103:aratim>2.0.co;2

Hong SY, Noh Y, Dudhia J (2006) A new vertical diffusion package with an explicit treatment of entrainment processes. Mon Weather Rev 134(9):2318–2341. doi:10.1175/mwr3199.1

Ishak A, Remesan R, Srivastava P, Islam T, Han DW (2013) Error correction modelling of wind speed through hydro-meteorological parameters and mesoscale model: a hybrid approach. Water Resour Manag 27(1):1–23. doi:10.1007/s11269-012-0130-1

Islam T, Rico-Ramirez MA, Han DW, Bray M, Srivastava PK (2013) Fuzzy logic based melting layer recognition from 3 GHz dual polarization radar: appraisal with NWP model and radio sounding observations. Theor Appl Climatol 112(1–2):317–338. doi:10.1007/s00704-012-0721-z

Islam T, Rico-Ramirez M, Srivastava P, Dai Q, Han D, Gupta M, Zhuo L (2014a) CLOUDET: a cloud detection and estimation algorithm for passive microwave imagers and sounders aided by naïve Bayes classifier and multilayer perceptron. IEEE Journal of Selected Topics in Applied Earth Observations and Remote Sensing PP (99)

Islam T, Rico-Ramirez MA, Han DW, Srivastava PK (2014b) Sensitivity associated with bright band/melting layer location on radar reflectivity correction for attenuation at C-band using differential propagation phase measurements. Atmos Res 135:143–158. doi:10.1016/j.atmosres.2013.09.003

Islam T, Srivastava P, Rico-Ramirez M, Dai Q, Gupta M, Singh S (2014c) Tracking a tropical cyclone through WRF–ARW simulation and sensitivity of model physics. Nat Hazards:1–23. doi:10.1007/s11069-014-1494-8

Islam T, Srivastava PK, Rico-Ramirez MA, Dai Q, Han DW, Gupta M (2014d) An exploratory investigation of an adaptive neuro fuzzy inference system (ANFIS) for estimating hydrometeors from TRMM/TMI in synergy with TRMM/PR. Atmos Res 145:57–68. doi:10.1016/j.atmosres.2014.03.019

Kain JS (2004) The kain-fritsch convective parameterization: an update. J Appl Meteorol 43(1):170–181. doi:10.1175/1520-0450(2004)043<0170:tkcpau>2.0.co;2

Milbrandt JA, Yau MK (2005a) A multimoment bulk microphysics parameterization. Part I: analysis of the role of the spectral shape parameter. J Atmos Sci 62(9):3051–3064. doi:10.1175/jas3534.1

Milbrandt JA, Yau MK (2005b) A multimoment bulk microphysics parameterization. Part II: a proposed three-moment closure and scheme description. J Atmos Sci 62(9):3065–3081. doi:10.1175/jas3535.1

Minnis P, Sun-Mack S, Young DF, Heck PW, Garber DP, Chen Y, Spangenberg DA, Arduini RF, Trepte QZ, Smith WL, Ayers JK, Gibson SC, Miller WF, Hong G, Chakrapani V, Takano Y, Liou KN, Xie Y, Yang P (2011) CERES edition-2 cloud property retrievals using TRMM VIRS and terra and aqua MODIS data-part I: algorithms. IEEE Trans Geosci Remote Sens 49(11):4374–4400. doi:10.1109/tgrs.2011.2144601

Nakanishi M, Niino H (2006) An improved mellor-yamada level-3 model: its numerical stability and application to a regional prediction of advection fog. Bound-Layer Meteorol 119(2):397–407. doi:10.1007/s10546-005-9030-8

Otkin JA, Greenwald TJ (2008) Comparison of WRF model-simulated and MODIS-derived cloud data. Mon Weather Rev 136(6):1957–1970. doi:10.1175/2007mwr2293.1

Platnick S, King MD, Ackerman SA, Menzel WP, Baum BA, Riedi JC, Frey RA (2003) The MODIS cloud products: algorithms and examples from terra. IEEE Trans Geosci Remote Sens 41(2):459–473. doi:10.1109/tgrs.2002.808301

Pleim JE (2007) A combined local and nonlocal closure model for the atmospheric boundary layer. Part I: model description and testing. J Appl Meteorol Climatol 46(9):1383–1395. doi:10.1175/jam2539.1

Skamarock WC, Klemp JB (2008) A time-split nonhydrostatic atmospheric model for weather research and forecasting applications. J Comput Phys 227(7):3465–3485. doi:10.1016/j.jcp.2007.01.037

Srivastava PK, Han DW, Rico-Ramirez MA, Al-Shrafany D, Islam T (2013) Data fusion techniques for improving soil moisture deficit using SMOS satellite and WRF-NOAH land surface model. Water Resour Manag 27(15):5069–5087. doi:10.1007/s11269-013-0452-7

Srivastava PK, Han D, Rico-Ramirez MA, O'Neill P, Islam T, Gupta M (2014a) Assessment of SMOS soil moisture retrieval parameters using tau–omega algorithms for soil moisture deficit estimation. Journal of Hydrology 519, Part A (0):574–587. doi:http://dx.doi.org/10.1016/j.jhydrol.2014.07.056

Srivastava PK, Han DW, Rico-Ramirez MA, Islam T (2014b) Sensitivity and uncertainty analysis of mesoscale model downscaled hydro-meteorological variables for discharge prediction. Hydrol Process 28(15):4419–4432. doi:10.1002/hyp.9946

Sukoriansky S, Galperin B, Perov V (2005) Application of a new spectral theory of stably stratified turbulence to the atmospheric boundary layer over sea ice. Bound-Layer Meteorol 117(2):231–257. doi:10.1007/s10546-004-6848-4

Tao WK, Simpson J, McCumber M (1989) An ice water saturation adjustment. Mon Weather Rev 117(1):231–235. doi:10.1175/1520-0493(1989)117<0231:aiwsa>2.0.co;2

Thompson G, Field PR, Rasmussen RM, Hall WD (2008) Explicit forecasts of winter precipitation using an improved bulk microphysics scheme. Part II: implementation of a new snow parameterization. Mon Weather Rev 136(12):5095–5115. doi:10.1175/2008mwr2387.1